Photon-mediated spin-polarized current in a quantum dot under thermal bias*

Feng Chi(迟锋)[1,†], Liming Liu(刘黎明)[1], and Lianliang Sun(孙连亮)[2]

[1] School of Electronic and Information Engineering, University of Electronic Science and Technology of China, Zhongshan Institute, Zhongshan 528400, China
[2] College of Science, North China University of Technology, Beijing 100041, China

(Received 22 October 2016; revised manuscript received 17 December 2016; published online 18 January 2017)

Spin-polarized current generated by thermal bias across a system composed of a quantum dot (QD) connected to metallic leads is studied in the presence of magnetic and photon fields. The current of a certain spin orientation vanishes when the dot level is aligned to the lead's chemical potential, resulting in a 100% spin-polarized current. The spin-resolved current also changes its sign at the two sides of the zero points. By tuning the system's parameters, spin-up and spin-down currents with equal strength may flow in opposite directions, which induces a pure spin current without the accompany of charge current. With the help of the thermal bias, both the strength and the direction of the spin-polarized current can be manipulated by tuning either the frequency or the intensity of the photon field, which is beyond the reach of the usual electric bias voltage.

Keywords: quantum dot, spin-polarized current, thermal bias, photon field

PACS: 73.21.La, 72.15.Jf, 73.50.Lw **DOI:** 10.1088/1674-1056/26/3/037304

1. Introduction

Spintronic devices utilize not only the charge degrees of freedom but also the spin degrees of freedom.[1–4] It is a hopeful candidate for a next-generation, energy-saving technology. The preparation and manipulation of spin-polarized current in a semiconductor quantum dot (QD), where quantized electron energy levels and electron number host, is at the heart of spintronics.[5–10] Many effective techniques have been developed besides the traditional ones heavily relying on the magnetic fields and magnetic materials. One of the most attractive breakthroughs is the spin Hall effect where electrons of different spin components are moving in opposite directions on the two edges of a sample in the presence of spin–orbit interactions.[11,12] Spin-up and spin-down electrons are then separated in different paths and the collisions between them are effectively suppressed. Consequently, fast speed and low energy consumption devices can be realized. Another spin control method is the time-dependent fields,[13] such as the laser field or microwave fields which allow for the preparation, manipulation, and readout of single electron spins in low-dimensional spintronic devices. Based on the optical pumping, laser cooling,[14] and photoluminescence polarization, a single spin state can be prepared in semiconductor QDs.[15] It can then be manipulated and detected in terms of oscillating magnetic field[16] and ultrafast optical pulses.[17] Similar to the generation of charge current by bias voltage, one can use spin bias[18] to prepare and manipulate spin-polarized current[19] and spin state in low-dimensional structures.[20–22]

Very recently, spin Seebeck effect has been observed in a metallic magnet, where a pure spin current or spin bias was induced by a temperature gradient across the system.[23] Such an effect may be used to generate and detect information encoded on electron spin in terms of thermal signals, which provides a new way of designing quantum devices based on the thermal bias instead of the usual electric bias. Many works have then been devoted to this thermospin effect in QD-based systems.[24–26] It was found that a spin-polarized current can be generated in a quite simple device due to the properties of the thermal bias and the quantized energy levels on the QD. In our previous work, we have demonstrated that a single spin state can be effectively prepared and manipulated in a QD coupled to ferromagnetic leads in the presence of a thermal bias.[27] Spin-polarized transport through a QD connected to a normal metal lead and a ferromagnetic lead held at different temperatures has been studied by Ying *et al.* using the master equation approach.[26] They found a rectification effect of the spin polarization, that is, in the positive temperature bias direction, the current polarization has a nonzero plateau, while the current polarization vanishes when the direction of the temperature bias is reversed. Impact of the time-dependent field on the electron transport through QDs has been investigated in several works with thermal bias.[28–32] Combined effects of polarized light and temperature difference on spin-polarized transport through a QD connected to two ferromagnetic electrodes have been studied by Ying *et al.*[28] A pure spin current can be obtained without being accompanied by charge current

*Project supported by the National Natural Science Foundation of China (Grant Nos. 61274101 and 51362031), the Initial Project for High-Level Talents of UESTC, Zhongshan Insitute, China (Grant No. 415YKQ02), and China Postdoctoral Science Foundation (Grant No. 2014M562301).

†Corresponding author. E-mail: chifeng@semi.ac.cn

© 2017 Chinese Physical Society and IOP Publishing Ltd

in such a system. Some new quantum phenomena, such as the sign reversal of the tunnel magnetoresistance, were found due to the temperature difference and the Rabi frequency.[28]

In the present paper, we study the associated effects of the photon field and the thermal bias on spin-dependent transport in a QD coupled to two normal metallic leads. Under a small thermal bias and a finite magnetic field, the current of a certain spin component has a zero point when its dot level is aligned to the chemical potential, whereas the current of the other spin component has a finite value due to the properties of the thermal bias. As a result, a 100% spin-polarized current emerges at this point denoted by the dot level which is adjustable by the gate voltage. Moreover, the spin-resolved current changes its sign at the two sides of the zero points, and then spin-up and spin-down currents may transport in opposite directions in some dot level regimes. If the current intensities of the two spin components are equal, the charge current vanishes, and there is a pure spin current whose polarization is infinite. To further manipulate the spin-polarized current, we apply a photon field on the system, and show that both the strength and the direction of the spin-polarized current are sensitive to either the photon strength or the photon frequency. We emphasize that the magnitude of the pure spin current is quite large compared to that in the previous work,[24] and the system is more favorable in experiment as there are no ferromagnetic electrodes, which were studied in Refs. [23]–[28].

2. Model and method

The considered system is described by the following Hamiltonian ($\hbar = 1$):[24]

$$H = \sum_{k,\sigma,\alpha=\mathrm{L,R}} \varepsilon_{k\alpha} c^{\dagger}_{k\alpha\sigma} c_{k\alpha\sigma} + \sum_{\sigma} \varepsilon_{\sigma}(t) d^{\dagger}_{\sigma} d_{\sigma} + \sum_{k,\sigma,\alpha=\mathrm{L,R}} (T_{k\alpha} c^{\dagger}_{k\alpha\sigma} d_{\sigma} + \mathrm{H.c.}), \quad (1)$$

where the first term describes the free electrons in the left (L) and right (R) leads, in which $c^{\dagger}_{k\alpha\sigma}$ ($c_{k\alpha\sigma}$) is the creation (annihilation) operator of an electron with momentum k, energy $\varepsilon_{k\alpha}$, and spin σ. We consider that the system is driven out of equilibrium by a thermal bias $\Delta T = T_{\mathrm{L}} - T_{\mathrm{R}}$, where $T_{\mathrm{L(R)}}$ is the temperature of the left (right) lead. The second term is for the electron on the QD, where $d^{\dagger}_{\sigma}$ (d_{σ}) is the creation (annihilation) operator of an electron with energy $\varepsilon_{\sigma}(t) = \varepsilon_d + \sigma g \mu_{\mathrm{B}} B/2 + \Delta \cos \Omega t$, with $\sigma = +$ and $\sigma = -$ denoting spin up and spin down, respectively. The quantity ε_d denotes the gate voltage tunable bare dot level, and B is the applied vertical magnetic field, with g and μ_{B} being the landé factor and the Bohr magneton, respectively. The Δ is the amplitude of the photon field, and Ω is the frequency of the photon. The last term describes the electron hopping between the QD and the leads with coupling strength $T_{k\alpha}$.

The time-dependent, spin-resolved current is calculated by following the standard Keldysh–Green's function technique:[33]

$$J_{\alpha\sigma}(t) = -e\langle \dot{N}_{\alpha\sigma} \rangle = -\mathrm{i}e\langle [H, N_{\alpha\sigma}] \rangle,$$

where $N_{\alpha\sigma}$ is the occupation number operator of lead α. Employing the equation of motion method, one finds the current in the following form:[33]

$$J_{\alpha\sigma}(t) = -e\Gamma_{\alpha} \int_{\infty}^{t} \mathrm{d}t_1 \int \frac{\mathrm{d}\varepsilon}{2\pi} \mathrm{Im}\{ \mathrm{e}^{-\mathrm{i}\varepsilon(t_1 - t)} \times [G^{<}_{\sigma}(t,t_1) + G^{\mathrm{r}}_{\sigma}(t,t_1) f_{\alpha}(\varepsilon)] \}, \quad (2)$$

where $f_{\alpha} = 1/\{1 + \exp[(\varepsilon - \mu_{\alpha})/k_{\mathrm{B}} T_{\alpha}]\}$ is the Fermi distribution function in lead α with chemical potential μ_{α} and temperature T_{α}. Here we assume zero electric bias voltage, i.e., $\mu_{\mathrm{L}} = \mu_{\mathrm{R}} = 0$, and the electron is driven by the thermal bias $\Delta T = T_{\mathrm{L}} - T_{\mathrm{R}}$ as mentioned above. The tunneling rate between lead α and the central region (QD) is given by $\Gamma_{\alpha} = 2\pi |T_{k\beta}|^2 \rho_{\alpha}$ with density of states ρ_{α} therein. The dot single-electron retarded and lesser Green's functions are defined respectively as $G^{\mathrm{r}}_{\sigma}(t,t_1) = -\mathrm{i}\theta(t-t_1)\langle \{ d_{\sigma}(t), d^{\dagger}_{\sigma}(t_1) \} \rangle$ and $G^{<}_{\sigma}(t,t_1) = \mathrm{i}\langle d^{\dagger}_{\sigma}(t_1) d_{\sigma}(t) \rangle$. Taking the time average of the current, one finds[33,34]

$$J_{\sigma} = e \int \frac{\mathrm{d}\varepsilon}{2\pi} [f_{\mathrm{L}}(\varepsilon) - f_{\mathrm{R}}(\varepsilon)] T_{\sigma}(\varepsilon), \quad (3)$$

with the transmission coefficient

$$T_{\sigma} = -\frac{\Gamma_{\mathrm{L}} \Gamma_{\mathrm{R}}}{\Gamma_{\mathrm{L}} + \Gamma_{\mathrm{R}}} \mathrm{Im} \sum_{n=-\infty}^{\infty} J_n^2 \left(\frac{\Delta}{\Omega} \right) G^{\mathrm{r}}_{n,\sigma}(\varepsilon), \quad (4)$$

where J_n is the n-th order Bessel function and the Fourier transform of the retarded Green's function is $G^{\mathrm{r}}_{n,\sigma}(\varepsilon) = [\varepsilon - (\varepsilon_{\mathrm{d}} + \sigma g \mu_{\mathrm{B}} B/2 + n\Omega) + \mathrm{i}(\Gamma_{\mathrm{L}} + \Gamma_{\mathrm{R}})/2]^{-1}$. The obtained Green's function indicates that the harmonic modulation of the dot level yields photon-assisted peaks in the transmission coefficient, and the peaks will arise in different dot levels ε_{d} due to the Zeeman splitting.

3. Numerical results

In numerical calculations, we assume symmetric barriers between the leads and the dots, and choose $\Gamma_{\mathrm{L}} = \Gamma_{\mathrm{R}} = \Gamma_0 = 1$ as the energy unit and set the constants $e = \hbar = k_{\mathrm{B}} = 1$. Throughout the paper, the system temperature in equilibrium state and the bias voltage $V = \mu_{\mathrm{L}} - \mu_{\mathrm{R}}$ are all fixed to zero, i.e., $T_0 = V = 0$. We also assume that the temperature of the left lead is higher than that of the right one, i.e., $T_{\mathrm{L}} = T_0 + \Delta T$ and $T_{\mathrm{R}} = T_0$, with fixed thermal bias $\Delta T = \Gamma_0$. Impacts of different values of T_0 and ΔT on the currents will be discussed qualitatively in the following. It should be noted that the size of the dot is an important factor. For example, it determines the electronic structures of the QDs, and changes the positions and the numbers of the dot levels on it. Correspondingly, the transport and the optoelectronic properties are significantly influenced.

In the present paper, we assume that the size of the dot is fixed for the sake of simplicity and the dot level can be controlled by the gate voltage. We first present in Fig. 1 the time-dependent conductance $G_\sigma(t)$ in the presence of the photon field, which is given by[33]

$$G_\sigma(t)=\frac{\Gamma_L\Gamma_R}{\Gamma_L+\Gamma_R}\mathrm{Im}\sum_{n=-\infty}^{\infty}\frac{\exp\left[-\mathrm{i}\frac{\Delta}{\Omega}\sin(\Omega t)\right]J_n(\frac{\Delta}{\Omega})\mathrm{e}^{\mathrm{i}k\omega t}}{\mu-\varepsilon_\sigma-k\Omega+\mathrm{i}(\Gamma_L+\Gamma_R)/2}. \quad (5)$$

It can be seen from the above equation that the positions of the resonant peaks in the spin-up and spin-down conductances will be split due to the Zeeman splitting of the dot level $\varepsilon_\sigma=\varepsilon_d+\sigma g\mu_B B/2$. Such a splitting can be enhanced by the photon field, and then it is possible to select a certain spin component to be transported through the system. Figures 1(a)–1(c) show that the conductance $G_\sigma(t)$ has a period of $2\pi/\Omega$ in unit of $1/\Gamma_0$ ($\hbar=1$). Meanwhile, both the strength and the lineshape of the conductance are influenced by the photon frequency. The properties of the conductance are also sensitive to the photon intensity as shown in Figs. 1(d)–1(f). It suggests that either the photon frequency or the photon intensity can effectively change the spin-dependent transport properties.

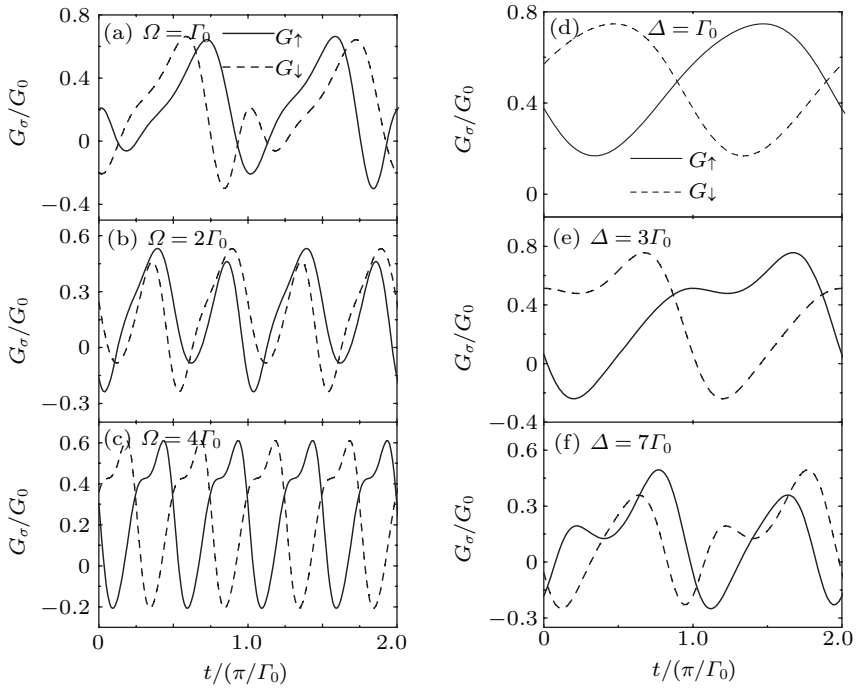


Fig. 1. Spin-dependent conductance G_σ versus time t for (a)–(c) different photon frequencies ω, and (d)–(f) different photon intensities. The bare dot level and the magnetic field are fixed to $\varepsilon_d=0$ and $g\mu_B B=2\Gamma_0$. The photon intensity in panels (a)–(c) is $\Delta=5\Gamma_0$. The photon frequency in panels (d)–(f) is $\omega=2\Gamma_0$.

Figure 2(a) presents the spin-resolved currents driven by the thermal bias free from the photon field. The dot level becomes spin-dependent due to the existence of the magnetic field, across which the current J_σ is zero. The properties of the electric current induced by the temperature difference can be explained as follows.[23,24,27,30] In the hotter lead, there are more electrons being excited above the chemical potential μ and correspondingly more holes being generated below μ. When the energy level ε_σ is below μ, the main carriers are holes and then the current J_σ is negative. When the energy level is above μ, the main carriers are electrons and thus the current is positive. When the dot level is aligned to the chemical potential, the current of the electrons is compensated by that of the holes and then the total current is zero. So one can tune the external gate voltage to obtain a certain anticipated spin-resolved current.

When the bare dot level ε_d locates within $\varepsilon_\uparrow$ and $\varepsilon_\downarrow$, $J_\uparrow$ and $J_\downarrow$ have opposite signs and then a large spin polarization is achieved. For example, when $\varepsilon_d=-\Gamma_0$, the spin-up level $\varepsilon_\uparrow=\varepsilon_d+g\mu_B B/2$ is aligned to the chemical potential μ, and then $J_\uparrow$ is zero but $J_\downarrow\neq 0$ as shown in Fig. 2(a). The current spin polarization $p=(J_\uparrow-J_\downarrow)/(J_\uparrow+J_\downarrow)$ equals -1. At $\varepsilon_d=\Gamma_0$, there is only a spin-up current and $p=1$. So the spin-up and spin-down currents are totally separated. At $\varepsilon_d=0$, the spin-up and spin-down currents with equal strength are flowing in opposite directions. Now the charge current $J_c=J_\uparrow+J_\downarrow$ is zero as indicated by the dashed line in Fig. 2(b), whereas the spin current $J_s=J_\uparrow-J_\downarrow$ achieves its maximum as shown by the solid line in the figure.

It is known that when a thermal bias ΔT is applied, the difference between the Fermi distributions of the left and right electrodes will drive a thermoelectric current at zero voltage bias.[23,24] This thermoelectric current induced by ΔT is fundamentally different from that driven by electric bias since the

latter is directly dominated by the properties at the Fermi level as shown in Fig. 2(c), while the former involves the full energy spectrum. Figure 2(c) presents the spin-dependent transmission (the solid and the dashed lines) and the difference between the Fermi functions in the left and right leads. The quantity $f_{\rm L}(\omega)-f_{\rm R}(\omega)$ changes its sign near the Fermi level $\mu=0$ (dotted line) and then the spin-dependent current, which is directly proportional to the product of T_σ and $f_{\rm L}(\omega)-f_{\rm R}(\omega)$, changes sign correspondingly.[29]

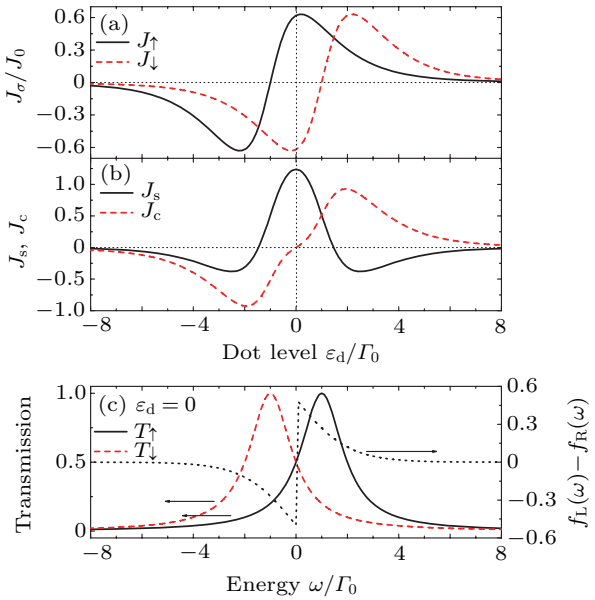


Fig. 2. (color online) (a) Spin-resolved current J_σ, (b) spin current, and (c) charge current as functions of the bare dot level $\varepsilon_{\rm d}$. The transmission coefficient and the difference between the Fermi functions of the two leads in panel (c) vary with the electron energy. The system is free from the photon field, and the magnetic field $g\mu_{\rm B}B=2\Gamma_0$, the thermal bias $k_{\rm B}\Delta T=\Gamma_0$.

In Fig. 3, we present the currents as functions of the bare dot level $\varepsilon_{\rm d}$ for different magnetic fields without photon field. With increasing magnetic field, the spin-up and spin-down levels are separated away accordingly, and then the positions of the zero points of the spin-dependent currents are varied as shown in Fig. 3(a). The line-shape of J_σ in the case of $g\mu_{\rm B}B=4\Gamma_0$ and $6\Gamma_0$ resembles that of $g\mu_{\rm B}B=2\Gamma_0$, whereas the characteristics of the charge current in Figs. 3(b) and 3(c) are drastically affected. Fortunately, the main characteristics of the currents near the chemical potential are qualitatively preserved due to the property of the thermal bias.[29] It is found that the charge current is always zero regardless of the variation of the magnetic field because the spin-up and spin-down currents with equal strength are flowing in opposite directions. As a result, there is always a large pure spin current at the chemical potential of the leads.

We now present in Fig. 4 the currents as functions of the photon frequency Ω and the bare dot level $\varepsilon_{\rm d}$ with fixed magnetic field and photon intensity. It is shown that the spin-up and spin-down currents are still zero at $\varepsilon_{\rm d}=-\Gamma_0$ in Fig. 4(a) and Γ_0 in Fig. 4(b). At the two sides of each zero point, J_σ changes its sign and develops a maximum. The spin current in Fig. 4(c) then has a maximum at the chemical potential, which is similar to the case of zero magnetic and photon fields. In the presence of the photon field, the dot level originally split by the magnetic field now becomes $\varepsilon_{\rm d}+\sigma\mu_{\rm B}B/2+n\Omega$ with $n=0,\pm1,\pm2,\pm3,\ldots$.[34] Correspondingly, the electrons will transport from the left lead to the right one whenever a photon-induced sub-channel enters into the conduction window opened by the thermal bias. Due to the Zeeman splitting of the dot level, each spin component electron enters into the conduction window at different photon frequency, resulting in an interesting frequency selective spin transport through the dot.[34]

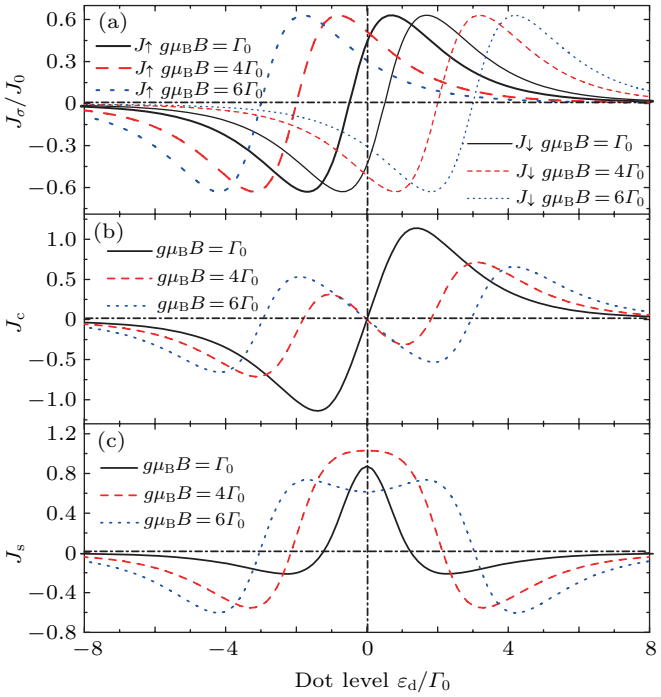


Fig. 3. (color online) (a) Spin-dependent current J_σ, (b) charge current $J_{\rm c}$, and (c) spin current $J_{\rm s}$ as functions of the bare dot level $\varepsilon_{\rm d}$ for different magnetic fields in the absence of the photon field.

The behavior of the photon-assisted current induced by the thermal bias, however, is quite different from that driven by the usual electric bias voltage.[34] The current develops peaks only in lower photon frequency regime in the case of the electric bias,[34] but the current J_σ develops peaks in both lower and higher frequency regimes ($n=\pm2,\pm3$) in our case as shown in Figs. 4(a) and 4(b). As discussed above, the reason is that the thermoelectric current induced by the thermal bias is determined by the full energy spectrum, whereas that driven by electric bias is directly dominated by the properties at the Fermi level. The spin current in Fig. 4(c) then has more resonant peaks, which offers extra opportunities for generating pure spin currents by selecting the photon frequency. As usual, the strength of the currents in these sub-channels is weakened with increasing n.[29–32,34]

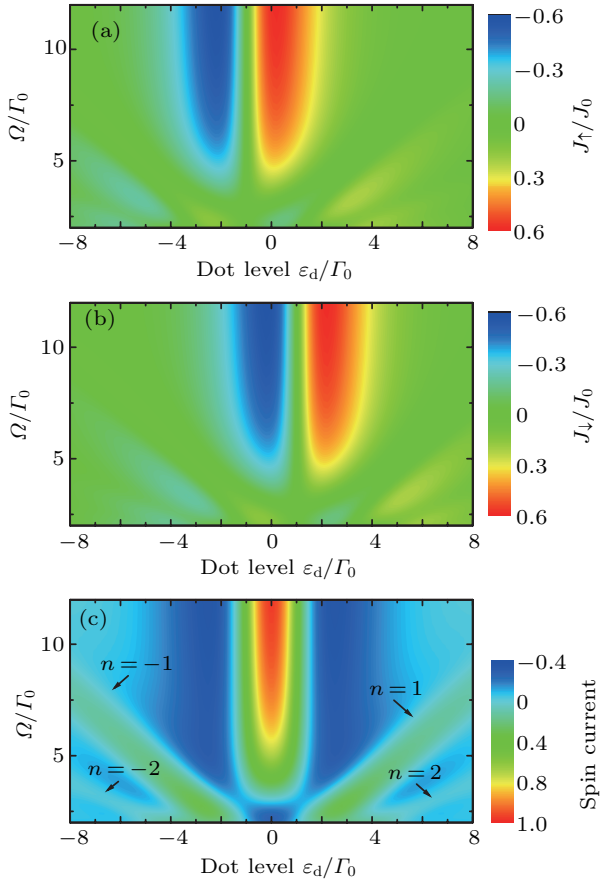


Fig. 4. (color online) (a), (b) Contour plots of the spin-dependent current J_σ. (c) Spin current J_s as a function of the bare dot level and the photon frequency. The magnetic field and the photon intensity are respectively set to be $g\mu_B B = 2\Gamma_0$ and $\Delta = 5\Gamma_0$.

Finally in Fig. 5, we investigate the pure spin current as a function of the photon frequency for different photon intensities when $\varepsilon_d = 0$. The strength of the pure spin current is sensitive to the photon intensity and is non-monotonically dependent on Δ. From Eq. (4), one can see that the transmission T_σ depends on not only the photon frequency but also the photon intensity. The photon frequency determines the location of the phonon-induced sub-channels and the phonon intensity affects the weight of the conduction ability of each sub-channel. In the higher frequency regime ($\Omega > 5\Gamma_0$), the spin current's strength decreases with increasing photon intensity since the photon-induced sub-channels are shifted away from $\varepsilon_d = 0$. Interestingly, in the lower frequency regime $\Omega < 5\Gamma_0$, either the strength or the direction of the pure spin current can be changed by varying the photon intensity. This is because now the interplay between the sub-channels is strong and then the intensities of the spin-up and spin-down currents are drastically changed. We emphasize that this can only happen under a thermal bias since now the currents are determined by the electrons in the full energy spectrum, whereas the current intensity in the presence of the electric current is only determined by the electron properties near the Fermi level.[34] In the present paper, we deal with the cases of fixed temperature T_0 and thermal bias ΔT. Generally, with increasing ΔT, the strength of the spin-polarized current will be enhanced accordingly with the properties obtained here quantitatively preserved. Increasing system temperature T_0, however, will weaken the function of the thermal bias and the working regimes for the spin-polarized currents will become unclear.

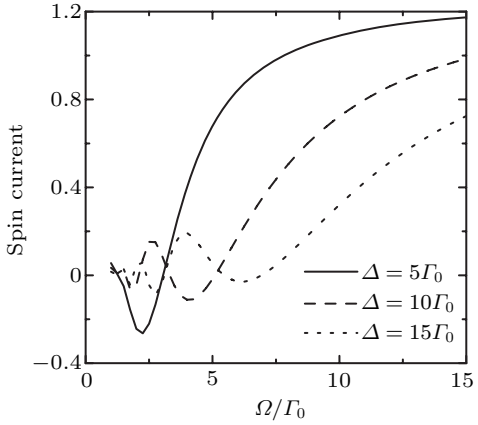


Fig. 5. Spin current as a function of the photon frequency for different photon intensities under fixed dot level $\varepsilon_d = 0$ and $g\mu_B B = 2\Gamma_0$.

4. Conclusion

We have studied the possibilities of generating and manipulating the spin-polarized current in a quantum dot coupled to normal metal leads in the presence of a thermal bias and a photon field. It is found that different from the current driven by the electric bias voltage, the spin-polarized current induced by the thermal bias has peaks in both lower and higher photon frequency regimes, providing additional work regimes for the pure spin current. Furthermore, both the strength and the direction of the pure spin current can be changed by varying either the photon frequency or the photon intensity. This is because the interplay between the spin-up and spin-down transmissions within the conduction window opened by the thermal bias is strong. We emphasize that the effects of the photon field on the spin-polarized current under thermal bias are quite different from the cases with electric bias, providing an effective spin control means based on thermospin technique.

References

[1] Prinz G A 1998 *Science* **282** 1660
[2] Hanson R, Kouwenhoven L P, Petta J R, Tarucha S and Vandersypen L M K 2007 *Rev. Mod. Phys.* **79** 1217
[3] Guo Y, Wang H, Gu B L and Kawazoe Y 2000 *Phys. Rev. B* **61** 1728
[4] Zhang Y T, Guo Y and Li Y C 2005 *Phys. Rev. B* **72** 125334
[5] Hanson R, Kouwenhoven L P, Petta J R, Tarucha S and Vandersypen L M K 2007 *Rev. Mod. Phys.* **79** 1217
[6] Liu P and Xiong S J 2009 *Chin. Phys. B* **18** 5414
[7] Chi F and Li S S 2005 *Chin. Phys. Lett.* **22** 2035
[8] Hou T, Wu S Q, Bi A H, Yang F B, Chen J F and Fan M 2009 *Chin. Phys. B* **18** 0783
[9] Wu S Q, Hou T, Zhao G P and Yu W L 2010 *Chin. Phys. B* **19** 047202
[10] Chi F, Sun L L, Huang L and Zhao J 2011 *Chin. Phys. B* **20** 017303
[11] Kato Y, Myers R C, Gossard A C and Awschalom D D 2004 *Science* **306** 5703
[12] Wunderlich J, Kaestner B, Sinova J and Jungwirth T 2005 *Phys. Rev. Lett.* **9** 4

[13] Mucciolo E R, Chamon C and Marcus C M 2002 *Phys. Rev. Lett.* **89** 146802
[14] Xu X D, Wu Y W, Sun B, Huang Q, Cheng J, Steel D G, Bracker A S, Gammon D, Emary C and Sham L J 2007 *Phys. Rev. Lett.* **99** 097401
[15] Ebbens A, Krizhanovskii D N, Tartakovskii A I, Pulizzi F, Wright T, Savelyev A V, Skolnick M S and Hopkinson M 2005 *Phys. Rev. B* **72** 073307
[16] Koppens F H L, Buizerk C, Tielrooij K J, Vink I T, Nowack K C, Meunier T, Kouwenhoven L P and Vandersypen L M K 2006 *Nature* **442** 766
[17] Clark S M, Fu K M C, Ladd T D and Yamamoto Y 2007 *Phys. Rev. Lett.* **99** 040501
[18] Frolov S M, Venkatesan A, Yu W, Folk J A and Wegscheider W 2009 *Phys. Rev. Lett.* **102** 116802
[19] Wang D K, Sun Q F and Guo H 2004 *Phys. Rev. B* **69** 205312
[20] Sun Q F, Xing Y X and Shen S Q 2008 *Phys. Rev. B* **77** 195313
[21] Lu H Z and Shen S Q 2008 *Phys. Rev. B* **77** 235309
[22] Chi F and Sun Q F 2010 *Phys. Rev. B* **81** 075310
[23] Uchida K, Takahashi S, Harii K, Ieda J, Koshibae W, Ando K, Maekawa S and Saitoh E 2008 *Nature* **455** 778
[24] Dubi Y and Di Ventra M 2009 *Phys. Rev. B* **79** 081302
[25] Qi F H, Yin Y B and Jin G J 2011 *Phys. Rev. B* **83** 075310
[26] Zhu L C, Jiang X D, Zu X T and Lü H F 2010 *Phys. Lett. A* **374** 4269
[27] Bai X F, Chi F, Zheng J and Li Y N 2012 *Chin. Phys. B* **21** 077301
[28] Ying Y B and Jin G J 2010 *Appl. Phys. Lett.* **96** 093104
[29] Chi F, Zheng J, Liu Y S and Guo Y 2012 *Appl. Phys. Lett.* **100** 233106
[30] Liu Y S, Yang X F, Chi F, Si M S and Guo Y 2012 *Appl. Phys. Lett.* **101** 213109
[31] Chen X B, Liu D P, Duan W H and Guo H 2013 *Phys. Rev. B* **87** 085427
[32] Tagani M B and Soleimani H R 2013 *J. Appl. Phys.* **113** 143709
[33] Jauho A P, Wingreen N S and Meir Y 1994 *Phys. Rev. B* **50** 5528
[34] Souza F M, Carrara T L and Vernek E 2011 *Phys. Rev. B* **84** 115322